materials proceedings

MDPI

Proceeding Paper

Water and Alkali Leaching for Simultaneous Iron and Alumina Separation from Hydrogen-Reduced Bauxite Residue-Calcite Pellets †

Manish Kumar Kar [1,*], Casper van der Eijk [2] and Jafar Safarian [1]

[1] Department of Materials Science and Engineering, Norwegian University of Science and Technology, Alfred Getz vei 2, 7491 Trondheim, Norway; jafar.safarian@ntnu.no
[2] Metal Production and Processing, SINTEF Industry, 7465 Trondheim, Norway; casper.eijk@sintef.no
* Correspondence: manish.k.kar@ntnu.no; Tel.: +47-96803633
† Presented at the 2nd International Conference on Raw Materials and Circular Economy "RawMat2023", Athens, Greece, 28 August–2 September 2023.

Abstract: Iron and alumina can be separated from bauxite residue and calcite self-hardened reduced pellets through simultaneous magnetic separation and alkali leaching. Bauxite residue and calcite self-hardened pellets were reduced non-isothermally by hydrogen gas to obtain metallic iron. Thereafter, the fine grounded reduced pellet powder was leached with a simultaneous magnetic stirrer, while two different leaching processes were applied. In a magnetic stirring alkali-leaching process, the simultaneous leaching and magnetic separation by Na_2CO_3 solution was carried out. In another process, the reduced pellets were leached into water with gradual magnetic separation followed by the addition of Na_2CO_3 solution. X-ray diffraction, scanning electron microscopy, X-ray fluorescence, and inductively coupled plasma mass spectroscopy were used to conduct phase analysis, microstructural analysis, compositional analysis, and elemental analysis of the leaching solutions, respectively. It was found that, there was an increase in iron in the magnetic fraction as compared to a nonmagnetic fraction in both the leaching processes; however, the iron recovery is more noticeable in the magnetic alkali leaching process. The recovery of alumina depends upon the amount of mayenite formation during reduction. The greater the amount of mayenite and the lower the amount of gehlenite, the greater the alumina recovery will be. The simultaneous alkali leaching and magnetic separation lead to greater unlocking of the reduced matrix and to greater iron and alumina recovery compared to magnetic water leaching followed by alkaline leaching.

Keywords: magnetic alkali leaching; non-isothermal; mayenite; gehlenite; magnetic separation

check for updates

Citation: Kar, M.K.; van der Eijk, C.; Safarian, J. Water and Alkali Leaching for Simultaneous Iron and Alumina Separation from Hydrogen-Reduced Bauxite Residue-Calcite Pellets. *Mater. Proc.* **2023**, *15*, 42. https://doi.org/10.3390/materproc2023015042

Academic Editors: Antonios Peppas, Christos Roumpos, Charalampos Vasilatos and Anthimos Xenidis

Published: 9 November 2023

Copyright: © 2023 by the authors. Licensee MDPI, Basel, Switzerland. This article is an open access article distributed under the terms and conditions of the Creative Commons Attribution (CC BY) license (https://creativecommons.org/licenses/by/4.0/).

1. Introduction

Aluminum is mainly produced from the electrolysis of alumina in the Hall–Heroult process. For the electrolysis process, the purity of alumina is above 99.9%, which is predominantly produced in the Bayer process [1]. During the processing of bauxite ore in the Bayer process, an undigested residue remains, which is known as red mud (the dewatered form is bauxite residue (BR)). Nearly 1–1.5 tons of BR is produced per ton of alumina, which also depends upon the mineralogical phases present and the processing parameters of the Bayer process [2]. The generation of BR is about 120 MT per annum, and till now, approximately 5 billion tons has been pilled globally [3–5]. There is no large-scale utilization of BR except for some usage in cement production [6]. A major fraction of BR consists of iron oxide and alumina. Recovery of iron and alumina from the BR will utilize a major fraction of this waste. Some of the studies have been carried out in the recovery of iron and alumina by using carbothermic reduction and leaching [7–9]; however, as the environmental concern about greenhouse gases is increasing, carbon is not a suitable reductant as per current and future scenarios. The substitution of hydrogen in place of

carbon, as a sustainable reductant, will generate water vapor during reduction instead of CO/CO_2 compared to carbothermic reduction, and therefore hydrogen used is of high interest to researchers.

There are few hydrogen reduction-related studies about iron and alumina recovery from BR. Iron and alumina recovery has been studied by Skibelid et al. (2022), and they studied the hydrogen reduction in BR-calcite sintered pellets at various temperatures followed by alkali leaching for alumina recovery. They found that at a reduction temperature of 1000 °C, all iron oxides were converted to metallic iron and the alumina recovery went above 87% during the alkali leaching [10]. An amount of alumina is lost in the form of complex phases such as gehlenite, which forms during the sintering and reduction of the pellets. The complete alumina recovery from mayenite by alkali leaching is restricted due to the formation of calcite. Azof et al. (2020) found that during the leaching of calcium aluminate slag with a Na_2CO_3 solution, the simultaneous formation of calcite is passivating the outer layer of the mayenite phase, which results in decreasing the reaction with increases in reaction time [11]. Due to the complete passivation of calcite around mayenite, the complete leachability of mayenite is hindered, which results in decreased alumina recovery.

From our previous work, during iron recovery by dry magnetic separation, there was less enrichment of the iron percentage in the separated magnetic fraction [12]. The low enrichment of iron in the magnetic fraction is due to the encapsulated matrix of iron and alumina, which results in both the presence of iron and alumina in the magnetic fraction. In another applied method, alumina was recovered from the reduced pellets after alkali leaching, followed by the magnetic separation of iron from the leaching residue, which was mostly composed of iron and calcite [10]. In this study, we tried to recover iron and alumina from the hydrogen-reduced BR-calcite pellets by employing simultaneous leaching and magnetic separation. The reduced pellets were leached by two different process schemes described in the next section.

2. Materials and Methods

2.1. Pelletizing and Hydrogen Reduction

BR, limestone, and quick lime were supplied from Mytilineos S.A., Marousi, Greece Greece (formerly known as Aluminum of Greece), Omya (Molde, Norway), and Nor-Frakalk(Verdal, Norway) respectively. These materials were received in agglomerated form. Materials were dried in an oven overnight at 80 ± 5 °C and deagglomerated to below 500 µm. BR, limestone, and quicklime were mixed in 65.4, 25.7, and 9.3 wt.%, respectively, in a tubular mixture. BR and calcium ($CaCO_3$ and CaO) were mixed in such a ratio so that it would form $CaO.Al_2O_3$, $2CaO.SiO_2$, and $CaO.TiO_2$ during the heat treatment process, which has been described in previous results [12]. In making self-hardened pellets a fraction of $CaCO_3$, is replaced with fine CaO to making use of the cementing nature of CaO, which gives strength to the pellets in the pelletization process and in the further aging process. The mechanism of hardening was described in our previous work [13]. After self-hardening, these pellets were dried in an oven to remove free moisture, then reduced in a vertical tube furnace by purging hydrogen gas from the bottom of the furnace. The schematic view and the furnace description are presented elsewhere [12].

The pellets were heated up to 200 °C in the presence of argon (1 NL/min) and then changed to H_2 gas during the heating up to the targeted temperature 1000 ± 10 °C with a heating rate of 20 °C/min and a flow rate of 4 NL/min H_2. After reaching the targeted temperature, hydrogen gas was purged for 120 min. The total mass loss (heating and reduction) during the heat treatment process was around 34 wt.% and the mass loss during the reduction in iron oxide to metallic iron was around 11 wt.%. The reduced pellets were ball milled for 30 min at 25 revolutions per minute (rpm). The particle size of the reduced pellets was around 8–10 µm (D_{50}), which was measured by a laser particle size analyzer.

2.2. Magnetic Leaching Process

The leaching experiment was performed inside an open glass beaker, which was heated by a hot plate with magnetic stirring. The schematic view of the leaching experiment is shown in Figure 1. The leaching experiments were conducted with a solid-to-liquid ratio of 1:10 and a solution concentration of 30 g Na_2CO_3/500 mL (distilled water). The leaching time was 120 min, with an overhead magnetic stirring speed of 400 rpm. After the leaching experiment was over, the leach residue and pregnant liquor were filtered using ashless grade filter paper. The leach residue was dried in an oven at 100 ± 5 °C overnight. The leaching setup and leaching parameter remained the same; however, the processes of leaching were different.

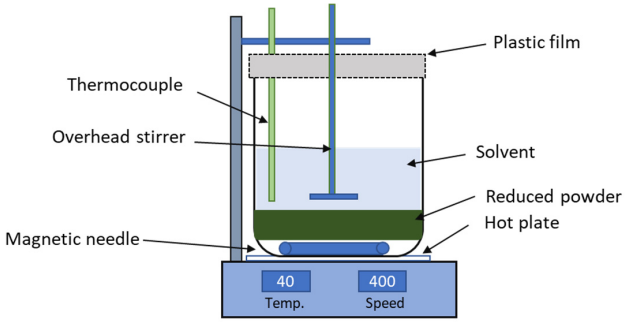

Figure 1. Schematic view of the setup for magnetic leaching.

In magnetic alkali leaching, the leaching solution was prepared with Na_2CO_3, then eventually a small amount of reduced powder was added, followed by the timely removal of magnetic fraction from the leaching solution via a magnetic needle. The process was repeated till the reduced power was finished and the magnetic separation was repeated for maximized separation of the magnetic fraction from the leaching residue. The frequency of the magnetic needle removal was 30 s, and this process was repeated several times. In the magnetic water leaching process, initially the grounded reduced pellet powder was leached with water gradually added in small amounts to 400 mL of distilled water. Similar to the previous process, the magnetic needle was removed after 30 s and the process was repeated to maximize the magnetic fraction recovery. Right after the water leaching and magnetic separation, 30 g Na_2CO_3 in 100 mL H_2O (the same concentration as the first leaching) was added, targeting a solid-to-liquid ratio of 1:10. The experimental flow sheet shown in Figure 2 provides information about the applied processes.

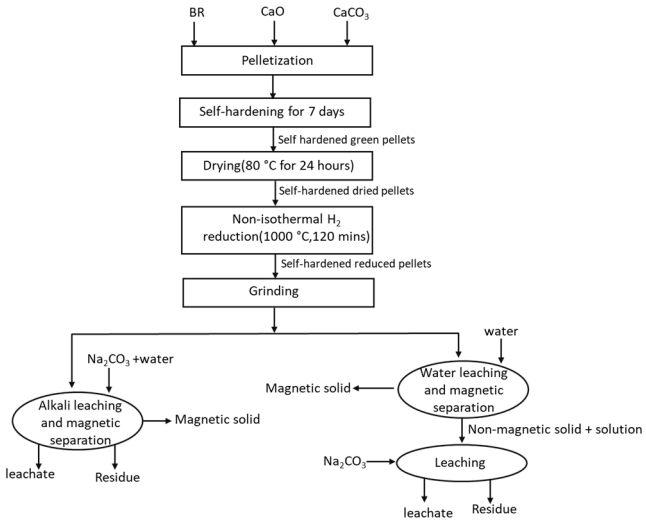

Figure 2. Experimental flow sheet of the process.

3. Results and Discussion

3.1. Phase Formation during Reduction and Leaching

The identified phases in the XRD spectrum of the self-hardened reduced pellets are shown in Figure 3. Mayenite ($Al_7Ca_6O_{16.49}$), iron, perovskite ($CaTiO_3$), larnite (Ca_2SiO_4), and lime (CaO) are the major phases found in the reduced pellets. There is no iron oxide present, which indicates that all iron oxide is reduced to metallic iron. Iron and mayenite have the most intense peaks. The formation of this compound happens in the solid state, so mass transport of the involved species is the dominating phenomena throughout Equations (1)–(3).

$$12CaO + 7Al_2O_3 \rightarrow Ca_{12}Al_{14}O_{33} \quad (1)$$

$$CaO + TiO_2 \rightarrow CaTiO_3 \quad (2)$$

$$2CaO + SiO_2 \rightarrow Ca_2SiO_4 \quad (3)$$

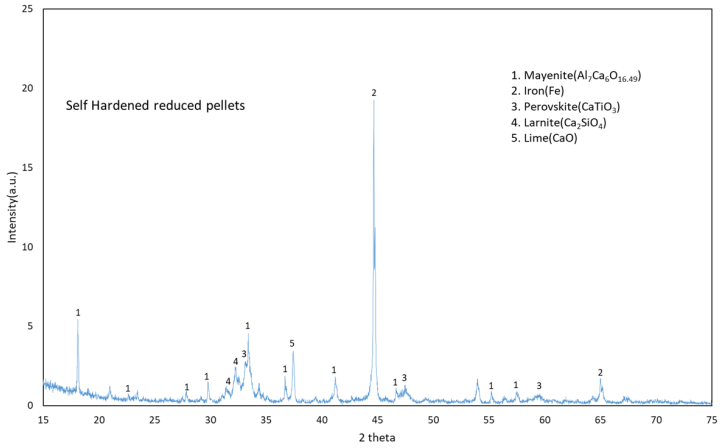

Figure 3. XRD analysis of self-hardened reduced pellet.

The identified phases in XRD spectra of magnetic and nonmagnetic fractions of solid residues in magnetic alkali leaching and magnetic water leaching of reduced pellets are shown in Figure 4. The phases present in both fractions are the same; however, the intensity of iron is higher in the magnetic fraction and calcite is higher in the nonmagnetic fraction. In the nonmagnetic fraction, the intensity of perovskite and the intensity of larnite are higher compared to the magnetic fraction.

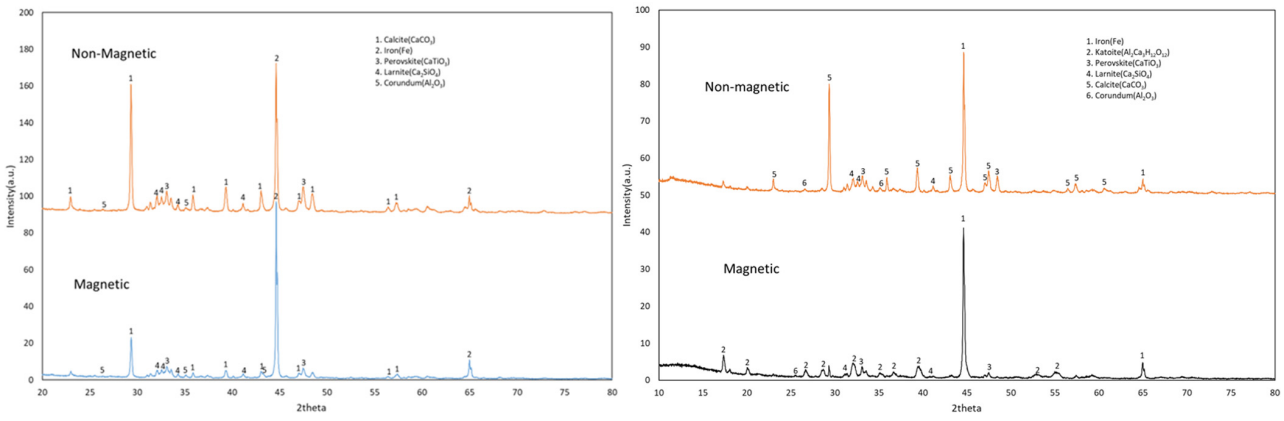

(a)XRD analysis magnetic alkali leaching (b)XRD analysis magnetic water leaching

Figure 4. XRD analysis results for magnetic and nonmagnetic fractions of (**a**) magnetic alkali leaching and (**b**) magnetic water leaching.

Iron and katoite comprise the major phase found in the magnetic fraction separated through water leaching; however, in the nonmagnetic fraction, calcite and iron were found, and most of the alumina are present in the katoite phase in the magnetic fraction.

3.2. Chemical Analysis

The elemental analysis is provided by XRF in the form of elemental analysis, but here we presented the most stable oxide forms of those elements. Additionally, iron is presented in elemental form as it was completely reduced, which is evidenced by XRD (Figure 3). As shown in Table 1, Fe wt.% in the separated magnetic fraction is highest in the magnetic alkali leaching. In the magnetic sample separated after water leaching followed by alkali addition, the alumina stays in both the magnetic and nonmagnetic fractions, whereas smaller amounts of alumina move to the leachate. In both the applied processes, calcium oxide is higher in the nonmagnetic fractions than in the magnetic portions. The iron present in reduced pellets was around 22 wt.% [12]; after magnetic alkali leaching, it increased to 43.5 wt.%, while, in the case of water leaching, the Fe content of the magnetic portion increased to 35.3 wt.%.

Table 1. XRF analysis of magnetic and nonmagnetic fractions of different types of leaching.

Oxides	Reduced Pellet	Magnetic Alkali Leaching		Magnetic Water Leaching	
		Magnetic	Nonmagnetic	Magnetic	Nonmagnetic
Na_2O	1.7	1.9	3.6	2.0	2.8
SiO_2	7.7	5.8	7.0	5.8	6.4
TiO_2	4.9	4.2	4.6	4.0	4.4
Al_2O_3	19.1	12.6	9.4	18.4	13.7
CaO	39.9	29.9	40.6	29.9	37.8
Fe	22.0	43.5	18.8	35.3	22.2
Other oxides	2.6	2.0	2.1	1.9	2.0
LOI	2.1	0.1	13.9	2.7	10.7
SUM	100.0	100.0	100.0	100.0	100.0

3.3. ICP-MS Analysis

As shown in Table 2, the aluminum concentration in the leachates is above 6000 mg/L for magnetic alkali leaching and it was about 4000 for the magnetic water alkali leaching. The silicon and iron concentrations were low for both the leaching processes. Obviously, more alumina has been leached during the magnetic alkali-leaching process.

Table 2. ICP-MS analysis of leachates after completed leaching practices (mg/L).

Sample (mg/L)	Na	Mg	Al	Si	P	S	K	Ca	Sc	Ti	V	Fe
Magnetic alkali leaching	28.964	<0.1	6035	138	2.25	41	48.8	7.01	<0.001	0.119	7.58	0.569
Magnetic Water alkali leaching	31.766	<0.1	3928	115	3.48	72	50.3	8.65	<0.001	0.359	6.31	2.37

3.4. Thermochemistry of Process and Reaction Mechanisms

During the Na_2CO_3 leaching process, Na^+ and $CO_3{}^{-2}$ from the bulk solution moved to the matrix interface, where the matrix is mostly composed of metallic iron and mayenite. Here, the assumption is that, in the reduced pellets along with metallic iron and mayenite, other phases such as perovskite and larnite are present; however, those phases are stable during alkali leaching [10]. The reaction of Na^+ with mayenite occurs on the surface of mayenite and $NaAlO_2$ is leached out from the pellets to the bulk solution, leaving behind $CaCO_3$ on the reduced pellets. The mechanism of $CaCO_3$ formation and growth was studied previously [14]. With the procession of leaching time, the $CaCO_3$ is accumulated over the particle surface, which leads to surface passivation. It has been shown that metallic iron is a stable phase in the process and hence during the leaching process, metallic Fe may

act similar to the other stable phases such as perovskite and larnite and therefore passivation via $CaCO_3$ deposition and growth occurs on the metallic iron particles. Since this calcite phase grows over the particle, it is separated by the magnet along with iron-containing particles and hence $CaCO_3$ was observed in Figure 4 in the XRD spectrum.

In the other leaching process, the reaction of mayenite with water occurs first and hydrated tricalcium aluminate is formed. As per the CaO-Al_2O_3-H_2O stability diagram, the leaching of mayenite with water gives $3CaO.Al_2O_3.6H_2O$ [15]. The reaction is mentioned below.

$$12CaO.7Al_2O_3 + 33H_2O \rightarrow 4[3CaO.Al_2O_3.6H_2O] + 3[Al_2O_3.3H_2O] \quad (4)$$

The magnetic separation during water leaching causes the separation of iron and katoite as the main components of this portion. After the separation of the magnetic portion and the addition of Na_2CO_3 into the system (nonmagnetic solid and solution), the dissolved alumina (in water) and the rest of the calcium aluminate in the solid are converted to aqueous $NaAlO_2$ while $CaCO_3$ is formed. Tricalcium aluminum hydroxide remains with the magnetic fraction, which increases the alumina and calcium content as compared to the magnetic alkali leaching, which is correlated with both the XRD and XRF results. As per the ICP-MS analysis, the aluminum concentration is low in the magnetic water-leaching process, which is due to the fact that a fraction of alumina is present in the form of tricalcium aluminate (katoite) in the magnetic fraction.

3.5. Alumina and Iron Recovery

The iron recovery, iron enrichment, and alumina recovery of the two leaching processes are presented in Table 3 as per the Equations (5)–(7), respectively. The iron and alumina recovery of the magnetic alkali leaching is higher than the magnetic water leaching followed by the addition of alkali. In the magnetic water leaching, alumina stays in the magnetic fraction as katoite, which decreases the alumina recovery and the relative iron fraction.

$$\%\ \text{Fe recovery} = \frac{[(\text{wt.\% Fe in magnetic}) \times \text{weight of magnetic fraction}(\%)]}{\text{wt.\% of Fe in reduced pellets}} \quad (5)$$

$$\text{Fe enrichment} = \frac{(\text{wt.\% Fe in magnetic fraction} - \text{wt.\% in reduced pellet})}{\text{wt.\% in reduced pellets}} \quad (6)$$

$$\%\ \text{alumina recovery} = \frac{\text{wt.\% alumina in Leachingsolution}}{\text{wt.\% alumina in reduced pellet}} \times 100 \quad (7)$$

Table 3. Iron recovery and alumina recovery and iron enrichment of two processes.

	Magnetic Alkali Leaching	Magnetic Water Leaching
% Fe recovery	63.33	57.79
% Fe enrichment	97.90	60.54
% Al_2O_3 recovery	63.00	40.70

4. Conclusions

The experimental work of magnetic alkali leaching, and magnetic water leaching followed by the addition of alkali of the reduced pellets is summarized as follows:

i. Direct alkali leaching of the reduced pellets lead to the passivation layer of $CaCO_3$ around the metallic iron particles.
ii. The alumina leaching was 63% in magnetic alkali leaching as compared to 41% in magnetic water leaching followed by the addition of alkali.
iii. During the water leaching, the mayenite converted to tricalcium aluminum hydrate ($3CaO.Al_2O_3.6H_2O$), which decreased the alumina recovery in the magnetic water-leaching process.

iv. The recovery of iron is 63.33% in the magnetic alkali-leaching processes as compared to 58% in magnetic water leaching. In magnetic water leaching subsequently addition of alkali; the formation of katoite during the water leaching process resulted in a higher concentration of alumina, calcium, in the magnetic fraction, leading to a reduction in alumina recovery.

v. In the magnetic alkali leaching process, the iron increased to 44 wt.% as compared to 22 wt.% in the reduced pellets and, in magnetic water leaching, it increased to 36 wt.% in the magnetic fraction.

Author Contributions: Conceptualization, M.K.K. and J.S.; methodology, M.K.K. and J.S.; software, M.K.K.; validation, M.K.K., J.S. and C.v.d.E.; formal analysis, M.K.K. and J.S.; investigation, M.K.K. and J.S.; resources, M.K.K., J.S. and C.v.d.E.; data curation, M.K.K. and J.S.; writing—original draft preparation, M.K.K.; writing—review and editing, M.K.K., J.S. and C.v.d.E.; visualization, M.K.K. and J.S.; supervision, J.S. and C.v.d.E.; project administration, J.S. and C.v.d.E.; funding acquisition, J.S. and C.v.d.E. All authors have read and agreed to the published version of the manuscript.

Funding: This research was funded by European Union's Horizon 2020 research and innovation program under grant number 958307.

Institutional Review Board Statement: Not applicable.

Informed Consent Statement: Not applicable.

Data Availability Statement: Data are available in this manuscript.

Conflicts of Interest: The authors declare no conflict of interest.

References

1. Habashi, F. *A Hundred Years of the Bayer Process for Alumina Production*; Springer: Berlin/Heidelberg, Germany, 2016; ISBN 3319485741.
2. Kumar, S.; Kumar, R.; Bandopadhyay, A. Innovative Methodologies for the Utilisation of Wastes from Metallurgical and Allied Industries. *Resour. Conserv. Recycl.* **2006**, *48*, 301–314. [CrossRef]
3. Wang, S.; Dube, B.; Vaughan, J.; Gao, S.; Peng, H. Silica Gel Free Region and Rare Earth Metal Extraction Correlations in Reprocessing Bauxite Residue. *Miner. Eng.* **2023**, *199*, 108115. [CrossRef]
4. Gräfe, M.; Power, G.; Klauber, C. Bauxite Residue Issues: III. Alkalinity and Associated Chemistry. *Hydrometallurgy* **2011**, *108*, 60–79. [CrossRef]
5. Power, G.; Gräfe, M.; Klauber, C. Bauxite Residue Issues: I. Current Management, Disposal and Storage Practices. *Hydrometallurgy* **2011**, *108*, 33–45. [CrossRef]
6. Pontikes, Y.; Angelopoulos, G.N. Bauxite Residue in Cement and Cementitious Applications: Current Status and a Possible Way Forward. *Resour. Conserv. Recycl.* **2013**, *73*, 53–63. [CrossRef]
7. Yin, P.T.; Buhle Xakalashe, B.F.; Panias, D.; Vassiliadou, V. Carbothermic Reduction of Bauxite Residue for Iron Recovery and Subsequent Aluminium Recovery from Slag Leaching. In Proceedings of the 35th International ICSOBA Conference, Hamburg, Germany, 2–5 October 2017; pp. 603–613.
8. Ekstrøm, K.E.; Bugten, A.V.; van Der Eijk, C.; Lazou, A.; Balomenos, E.; Tranell, G. Recovery of Iron and Aluminum from Bauxite Residue by Carbothermic Reduction and Slag Leaching. *J. Sustain. Metall.* **2021**, *7*, 1314–1326. [CrossRef]
9. Anawati, J.; Azimi, G. Integrated Carbothermic Smelting–Acid Baking–Water Leaching Process for Extraction of Scandium, Aluminum, and Iron from Bauxite Residue. *J. Clean. Prod.* **2021**, *330*, 129905. [CrossRef]
10. Skibelid, O.B.; Velle, S.O.; Vollan, F.; Van der Eijk, C.; Hoseinpur-Kermani, A.; Safarian, J. Isothermal Hydrogen Reduction of a Lime-Added Bauxite Residue Agglomerate at Elevated Temperatures for Iron and Alumina Recovery. *Materials* **2022**, *15*, 6012. [CrossRef] [PubMed]
11. Azof, F.I.; Safarian, J. Leaching Kinetics and Mechanism of Slag Produced from Smelting-Reduction of Bauxite for Alumina Recovery. *Hydrometallurgy* **2020**, *195*, 105388. [CrossRef]
12. Hassanzadeh, A.; Kar, M.K.; Safarian, J.; Kowalczuk, P.B. An Investigation on Reduction of Calcium Added Bauxite Residue Pellets by Hydrogen and Iron Recovery through Physical Separation Methods. *Metals* **2023**, *13*, 946. [CrossRef]
13. Kar, M.K.; Van Der Eijk, C.; Safarian, J. Hydrogen Reduction of High Temperature Sintered and Self-Hardened Pellets of Bauxite Residue Produced via the Addition of Limestone and Quicklime. In Proceedings of the 40th International ICSOBA Conference, Athens, Greece, 10–14 October 2022; p. 11.

14. Azof, F.I.; Kolbeinsen, L.; Safarian, J. Kinetics of the Leaching of Alumina-Containing Slag for Alumina Recovery. In Proceedings of the European Metallurgical Conference, Düsseldorf, Germany, 23–26 June 2019; GDMB Verlag GmbH: Clausthal-Zellerfeld, Germany, 2019; Volume 2.
15. Lothenbach, B.; Pelletier-Chaignat, L.; Winnefeld, F. Stability in the System $CaO–Al_2O_3–H_2O$. *Cem. Concr. Res.* **2012**, *42*, 1621–1634. [CrossRef]

Disclaimer/Publisher's Note: The statements, opinions and data contained in all publications are solely those of the individual author(s) and contributor(s) and not of MDPI and/or the editor(s). MDPI and/or the editor(s) disclaim responsibility for any injury to people or property resulting from any ideas, methods, instructions or products referred to in the content.